REPORT DOCUMENTATION PAGE

Form Approved
OMB No. 0704-0188

1. REPORT DATE *(DD-MM-YYYY)*	**2. REPORT TYPE**	**3. DATES COVERED** *(From - To)*
09/03/2012	FINAL PERFORMANCE REPORT	7/01/2009-5/31/2012

4. TITLE AND SUBTITLE

Influence of Grain Structure and Doping on the Deformation and Fracture of Polycrystalline Silicon for MEMS and NEMS

5a. CONTRACT NUMBER

5b. GRANT NUMBER
FA9550-09-1-0535

5c. PROGRAM ELEMENT NUMBER

6. AUTHOR(S) IOANNIS CHASIOTIS

Aerospace Engineering, U. Illinois at Urbana-Champaign, M/C 236
306 Talbot Lab, 104 South Wright St., Urbana, IL 61801

5d. PROJECT NUMBER

5e. TASK NUMBER

5f. WORK UNIT NUMBER

7. PERFORMING ORGANIZATION NAME(S) AND ADDRESS(ES)

UNIVERSITY OF ILLINOIS
Aerospace Engineering
104 South Wright St.
Urbana, IL 61801

8. PERFORMING ORGANIZATION REPORT NUMBER

9. SPONSORING / MONITORING AGENCY NAME(S) AND ADDRESS(ES)

Air Force Office of
Scientific Research (AFOSR)
Program: Mechanics of
Multifunctional Materials and
Microsystems

10. SPONSOR/MONITOR'S ACRONYM(S)
Program Manager:
Dr. B.L. Lee

11. SPONSOR/MONITOR'S REPORT NUMBER(S)
AFRL-OSR-VA-TR-2012-1168

12. DISTRIBUTION / AVAILABILITY STATEMENT

Approved for public release

13. SUPPLEMENTARY NOTES

14. ABSTRACT

This research program investigated the effect of microstructure and doping on the effective mode I critical stress intensity factor, $K_{IC,eff}$, and the tensile strength of 1-μm thick films comprised of columnar or laminated polysilicon doped with different concentrations of Phosphorus. The $K_{IC,eff}$ was 0.8-1.2 MPa√m and differed by as much as 25% for specimens with specific grain size and doping concentration. This data scatter was attributed to differences in the local material details at the location of the crack tip. The $K_{IC,eff}$ of columnar polysilicon was generally higher than laminated polysilicon, but the latter demonstrated smaller variability in $K_{IC,eff}$, due to the averaging effect of the laminate structure. The tensile strengths of undoped columnar and laminated polysilicon were 1.28±0.06 GPa and 2.28±0.15 GPa, respectively. While high doping impacted the strength of the former, it had negligible effect on the strength of the latter. It was concluded that microstructural control of failure initiation is compromised by large defects that are due to post processing, and that laminated polysilicon films do improve on the consistency and magnitude of film strength. It was also shown that the Weibull parameters derived from the larger specimens could predict the characteristic strengths of ~200 times smaller specimens for different film structures and doping conditions, and *vice versa*.

UNIVERSITY OF ILLINOIS
AEROSPACE ENGINEERING

FINAL PERFORMANCE REPORT

Reporting Period: 7/01/2009 - 5/31/2012

Influence of Grain Structure and Doping on the Deformation and Fracture of Polycrystalline Silicon for MEMS and NEMS

PI: Ioannis Chasiotis

Aerospace Engineering
University of Illinois at Urbana-Champaign
Talbot Lab, 104 S. Wright Street, Urbana, IL 61801
Telephone: (217) 244-1474, Fax: (217) 244-0720, E-mail: chasioti@illinois.edu

AFOSR GRANT # FA9550-09-1-0535

Program Manager: Dr. B.L. Lee

SEPTEMBER 2012

15. SUBJECT TERMS					
16. SECURITY CLASSIFICATION OF:			17. LIMITATION OF ABSTRACT	18. NUMBER OF PAGES	19a. NAME OF RESPONSIBLE PERSON Ioannis Chasiotis
a. REPORT unclassified	b. ABSTRACT unclassified	c. THIS PAGE unclassified		25	19b. TELEPHONE NUMBER *(include area code) (217) –244-1474*

Standard Form 298 (Rev. 8-98)
Prescribed by ANSI Std. Z39.18

Acknowledgements

The PI and his graduate students supported by this program gratefully acknowledge the support by the Air Force Office of Scientific Research (AFOSR) through grant FA9550-09-1-0535 and Dr. B.L. Lee as the program manager. The authors thank their collaborator Dr. Brad Boyce of the Sandia National Laboratories for providing the samples for the work conducted under this research grant.

DETAILED DESCRIPTION OF RESEARCH

I. PROBLEM STATEMENT AND SCIENTIFIC RELEVANCE

Polysilicon has been one of the most common materials for Microelectromechanical Systems (MEMS) because of its advantageous electrical and mechanical properties as well as the mature processes for the fabrication of intricate devices [1]. MEMS perform best as suspended two-dimensional devices that contain slender features that allow for large in-plane displacements under relatively low forces. These components, however, are subjected to large stresses that often exceed 1-2 GPa in order to reach the desired motion. The brittle nature of polysilicon MEMS presents the advantage of dimensional stability but raises the concern of catastrophic fracture due to voids, crevices or micro cracks on the surface or the volume of the material comprising a device [2]. Metrics, such as tensile strength and fracture toughness needs to be related to individual processing steps to determine the limiting fabrication processes and develop predictive tools for device reliability as a function of fabrication routes.

Given the direct dependence of fracture on flaw size, such as surface roughness and micro defects introduced during bulk micromachining, single crystal silicon has been shown to exhibit fracture strength in the range of 1-20 GPa [3,4]. Given its granular microstructure, the strength of polycrystalline silicon is limited in an even smaller range of 1-5 GPa [5-10]. In both cases, the mechanical strength is dependent on specimen size [2,8,11]. Past research has shown that Reactive Ion Etching (RIE), deposition and doping influence the surface roughness [12] and are among the primary sources of catastrophic flaws. Furthermore in the presence of metallization layers, it has been shown that the mechanical strength can be strongly affected by the extent and nature of the sacrificial etching process [13-15]. Other microstructures, such as laminated polysilicon or amorphous silicon, have been shown to resist failure until 9.7 GPa compared to 5 GPa for columnar polysilicon [16]. The difference in fracture strength was attributed to fewer process related flaws present on the free surface of polysilicon films. On the contrary, Tsuchiya et al [17] reported the strength of amorphous silicon to be lesser than that of polysilicon which they attributed to the presence of 0.4% atomic hydrogen and large defects. They also noticed that the strength of polysilicon depended on the annealing temperature that in turn dictated the grain size. While the grain size did not directly impact the fracture strength, the size of defects formed was bigger in the case of polysilicon with large grains due to processing conditions and hence displayed a lower strength compared to small grain polysilicon that had 50% smaller in size defects.

The resistance of a material to fracture can be quantified independently of the flaw size via fracture experiments with pre-existing sharp cracks. A reference to the expected values for the critical stress intensity factor is provided by single crystal silicon [18-21], which can be as low as 0.82 MPa√m for (111) planes [19], and as high as 1.22 MPa√m according to [18]. More specifically, the critical stress intensity factor of single crystal silicon of (100), (110) and (111) was reported as 0.95 MPa√m, 0.90 MPa√m and 0.83 MPa√m respectively [19]. The values of the critical stress intensity factor of polysilicon films have been reported by several groups [22,23], with the most recent reports providing distributions of values in the range of 0.8-1.2 MPa√m [24,25], where the variation in values was attributed to local material anisotropy near the crack tip and grain heterogeneity. A direct consequence of this distribution of values for the

effective critical stress intensity factor is that cracks may, in some cases, arrest as long as the effective mode I stress intensity is less than 1.2 MPa√m [24], potentially leading to an R-curve behavior. Furthermore, in a computational cohesive-zone analysis, Foulk *et al* [26, 27] demonstrated that the grain shape, crystal lattice orientation and grain boundary strength could increase the apparent critical stress intensity factor by local crack tip deflection and grain bridging. Thus modification of the grain structure could affect the resistance of polysilicon to crack growth. Additionally, Boron or Phosphorous dopants are known to segregate to grain boundaries but their effect on toughening and strengthening has been elusive [28,29]: Zeng *et al* [28] reported a 3% increase in the critical stress intensity factor of silicon that is heavily doped with P, while Swadener *et al* [29] reported an equally insignificant effect of doping. However if grain boundaries and triple junction points can influence the crack tip path and hence the effective critical stress intensity factor, influencing the cohesive strength of grain boundaries via doping may provide an additional tool to control crack initiation and arrest.

In this project we investigated the effect of microstructure and doping on the strength and the critical stress intensity factor of polysilicon with custom microstructure fabricated in an experimental run at the Sandia National Laboratories. The mechanical properties of polysilicon manufactured by the regular SUMMiT V^{TM} process by the Sandia National Laboratories have been reported before by Chasiotis and Knauss [5] and Boyce *et al* [8] and who identified the sidewall roughness as the location of flaws controlling failure. In this project a new microstructure has been explored, in which a polysilicon structural layer has been substituted by a laminated structure to reduce the grain size and consequently the maximum flaw size. A first report on this material by Boyce *et al* [30] reported a 60-90% increase in fracture strength for laminated polysilicon compared to columnar polysilicon. One of the key questions that remained after that early work was whether the improvement in strength was entirely attributable to differences in flaw size, or if the doping and microstructure also influenced the material's fracture toughness. This project investigated the effect of grain structure and doping on the local fracture behavior of this new polysilicon which was quantified by fracture experiments with sharp cracks. Furthermore, mechanical strength measurements with specimens at least 100 times larger than those used in [30] where carried out to investigate the dependency of strength parameters on specimen size which is important for device design.

II. EXPERIMENTAL METHODS

II.a Materials and Fabrication Methods

Two types of 1-μm thick polysilicon specimens were fabricated for this project: Specimens with grain size of 285 nm, which is somewhat smaller than the standard SUMMiT V^{TM} microfabrication process [31], and specimens with laminated structure and grain size of 125 nm. The grain structure of the former polysilicon was columnar and henceforth we refer to it as "columnar polysilicon" while the latter polysilicon with finer grain size of 125 nm will be referred to as "laminated polysilicon". To produce the two different microstructures, a custom polysilicon fabrication run was performed at the Sandia National Laboratories. The initial processing steps were identical for both microstructures. First, a 0.63 μm thick oxide layer was thermally grown on the silicon wafer followed by 0.8 μm thick low–stress nitride layer using LPCVD. These blanket films act as electric insulating layers between the wafer and operating MEMS structures. A 0.3-μm thick LPCVD polysilicon (Poly0) layer was deposited on top of the nitride layer as a ground layer. A 2 μm thick sacrificial oxide layer (SacOx1) of either phosphosilicate glass (PSG) with 0.5% or 2% P or undoped silane glass was then deposited and patterned. Thus, each type of polysilicon was doped at two concentration levels with P. Subsequently, a 1-μm thick columnar polysilicon layer (Poly1) was deposited in a furnace at 580 °C. The laminated polysilicon was fabricated by depositing 10 alternate layers of 100 nm thick amorphous and polycrystalline silicon resulting in a 1 μm thick composite. A second sacrificial oxide layer (SacOx2) was deposited on top of Poly1 and was chemo-mechanically planarized to a thickness of 2 μm. The wafers were then annealed in N_2 environment for 1hr and at 1050 °C to allow for diffusion of P. In the case of laminated polysilicon, the amorphous silicon became polycrystalline during annealing and resulted in the laminated structure shown in Figure 1(c). Further details on the processing methods, the resulting grain structures, and preliminary strength measurements are provided in [30].

A top view of a microfabricated polysilicon tensile specimen is shown in Figure 1(a) and a cross-sectional SEM image of columnar and laminated polysilicon is shown in Figures 1(b) and 1(c), respectively. The uniaxial tension specimens were 100 μm wide with a gage length of 1,000 μm. Sharp cracks were introduced into the specimen gauge section by a microhardness indenter as described in [24]. Using this method, indentation was performed close to specimen edge on the substrate and the edge cracks emanating from the indent propagated into the tensile polysilicon specimen through sacrificial oxide layer. SEM and AFM photographs of the crack tips were obtained for each specimen to measure the crack length and obtain the precise location of the crack tip. Figure 2 shows the SEM and AFM images of a crack and its tip, respectively, in undoped columnar and laminated polysilicon. After indentation, the films were etched in 49% HF to obtain freestanding specimens for fracture experiments. Specimens without pre-cracks were used to measure the material fracture strength.

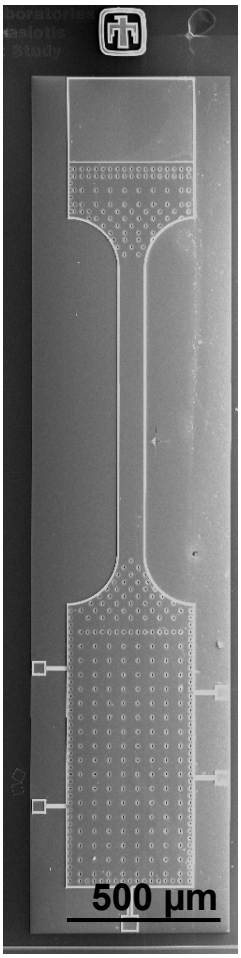

(a)

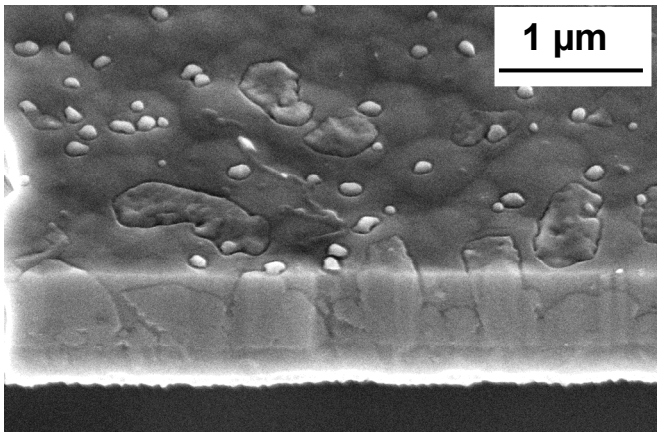

(b)

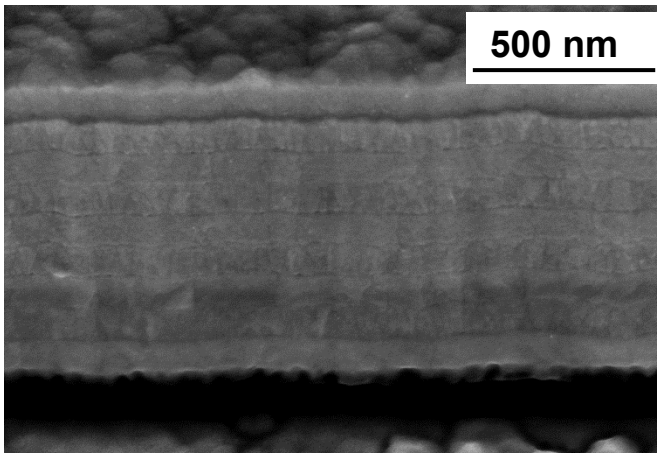

(c)

Figure 1. (a) Uniaxial tension specimen, and cross sectional view of **(b)** columnar and, **(c)** laminated polysilicon.

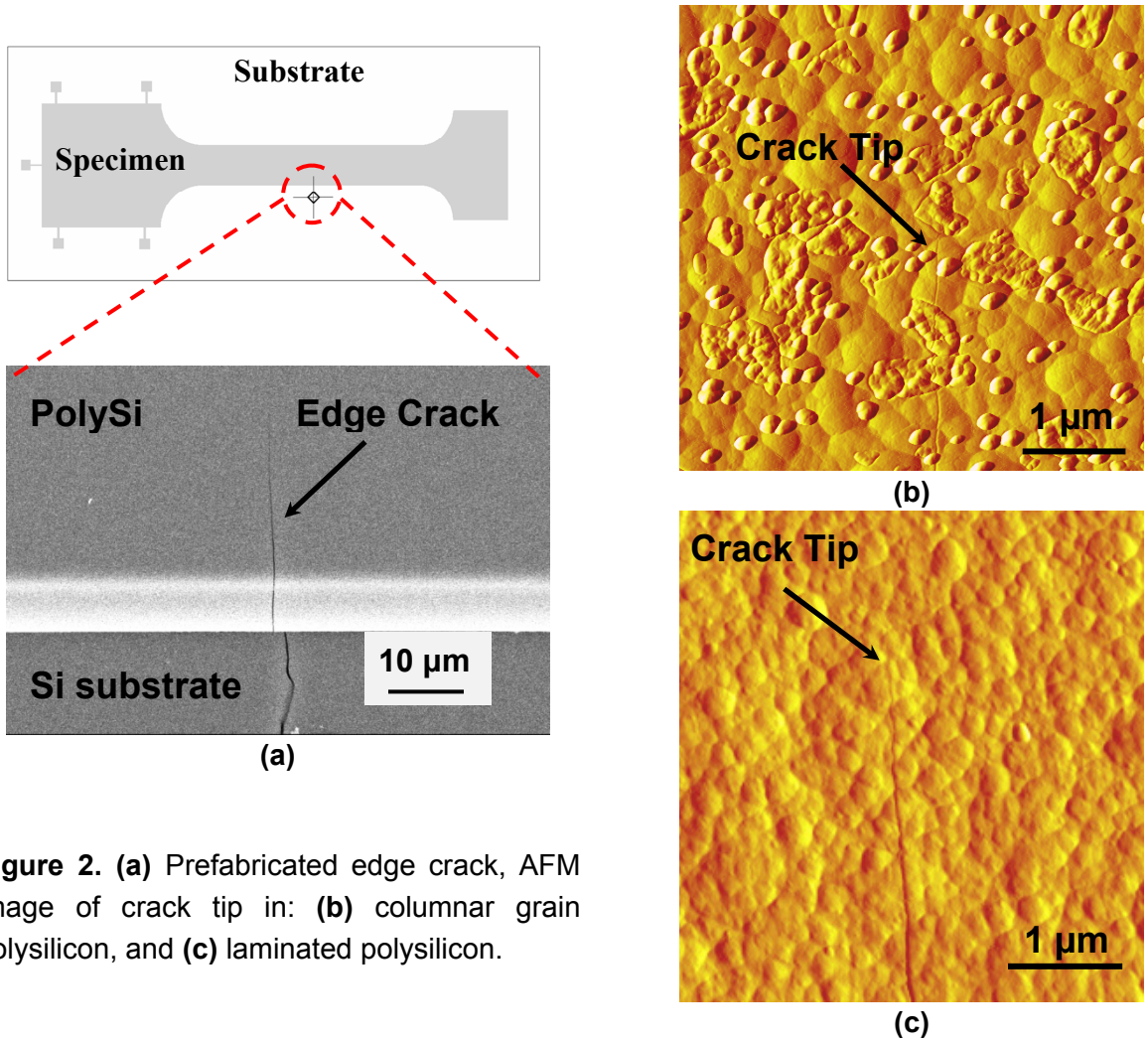

Figure 2. (a) Prefabricated edge crack, AFM image of crack tip in: **(b)** columnar grain polysilicon, and **(c)** laminated polysilicon.

II.b Fracture and Tensile Strength Experiments

The experimental apparatus for the strength and fracture experiments was described in previous reports [32]. In this experimental technique, the specimen ends are gripped to loadcell and PZT actuator mounted on three dimensional micro-positioners that facilitates loading in uniaxial tension. The specimens were loaded until failure at a strain rate of 6×10^{-4} s^{-1} and the force was recorded by a small force loadcell. The mode I critical stress intensity factor of the edge cracked specimens was calculated using an existing solution derived for LEFM [33] as given by Equation (1), where σ_∞ is far field stress in the specimen, a is crack length and Y is shape function calculated using Equation (2) where w is width of the specimen. The thickness of the specimens was measured from their fracture cross section imaged using SEM, which was in good agreement with the nominal values calculated using deposition rates and times.

$$K_{Ic} = \sigma_{\infty} Y \sqrt{\pi a} \tag{1}$$

$$Y = 1.122 - 0.231\left(\frac{a}{w}\right) + 10.55\left(\frac{a}{w}\right)^2 - 21.71\left(\frac{a}{w}\right)^3 + 30.382\left(\frac{a}{w}\right)^4 + HOT \tag{2}$$

Finally, the fracture strength was measured using uniform tension specimens as shown in Figure 1(a), which did not have an edge crack.

III. RESULTS

The $K_{IC,eff}$ and fracture strength for columnar and laminated polysilicon thin films doped with different concentrations of Phosphorous are given in Table 1 and shown in Figure 3. A minimum of 15 specimens were tested for each specimen kind. The $K_{IC,eff}$ of all the polysilicon thin films was in the range of 0.8-1.2 MPa√m which agrees with the range of K_{IC} values for bulk silicon [18-20] and the $K_{IC,eff}$ for polysilicon fabricated by a different process (MUMPS) previously reported by this group [24,25]. The average $K_{IC,eff}$ varied slightly with grain structure and with doping level. Specifically, the $K_{IC,eff}$ values for columnar polysilicon were in the range of 0.88–1.2 MPa√m and were slightly higher than those of laminated polysilicon that were in the range of 0.85-1.08 MPa√m, averaging 0.95±0.08 MPa√m and 0.99±0.05 MPa√m, respectively. More substantial was the sample-to-sample scatter in fracture toughness: within a given material, microstructure, and doping level, there was significant variability in fracture toughness. For example, two specimens that belonged to same die exhibited $K_{IC,eff}$ values that differed by as much as 40%. The scatter in effective critical stress intensity factor values was larger in the case of columnar polysilicon doped with 0.5% and 2% PSG compared to laminated polysilicon.

Table 1. Mode I critical stress intensity factor and tensile strength of columnar grain and laminated polysilicon doped with different concentrations of P. The data are the mean and standard deviation of measured values.

Specimen type	$K_{IC,eff}$ (MPa√m)	Failure strength (GPa)
Undoped, Laminated	0.99±0.05	2.32±0.15
0.5% PSG, Laminated	0.94±0.10	
2% PSG, Laminated	0.95±0.08	2.46±0.22
Undoped, Columnar	0.95±0.08	1.30±0.09
0.5% PSG, Columnar	1.02±0.13	
2% PSG, Columnar	1.05±0.14	0.95±0.07

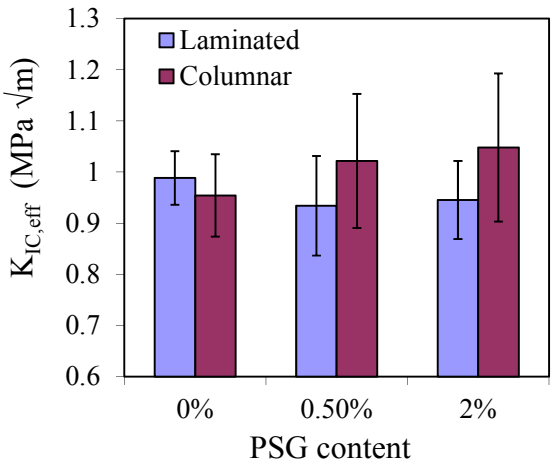

Figure 3. $K_{IC,eff}$ for laminated and columnar grain polysilicon vs. P doping. The bar graphs represent mean and standard deviation of the measured values.

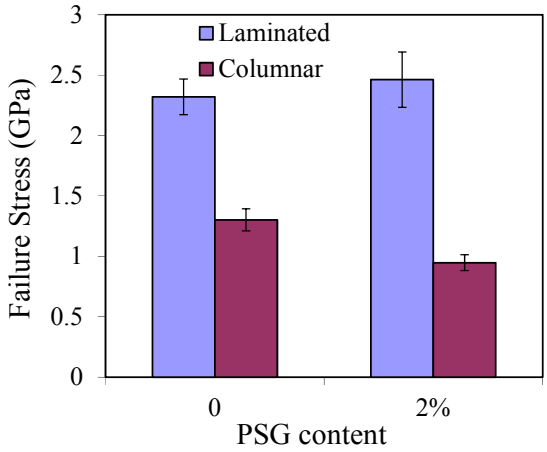

Figure 4. Failure stress of columnar and laminated polysilicon grains that were doped with 0% and 2% P. The bar graphs represent mean and standard deviation of the measured values.

The fracture strength measurements are shown in Figure 4. The average strength of columnar polysilicon was 1.28±0.06 GPa and was 44% lower than that of the laminated polysilicon that was measured as 2.28±0.14 GPa. While the strength of columnar polysilicon doped with 2% PSG dropped to 0.99±0.48 GPa, i.e. 23% lower than the undoped material, the strength of laminated polysilicon did not change significantly with doping.

Due to the brittle nature of polysilicon and its high strength, the specimens shattered upon failure and hence, post fracture analysis of the cross sections could not be carried out. The tensile strength depends on the flaws that formed during fabrication such as voids, micro-cracks, and surface roughness. The statistical dependence of strength on specimen size was quantified by using the Weibull distribution function [34]. The cumulative probability function for the three-parameter Weibull distribution for uniform tension is given by Equation (3), where σ_u is the threshold stress below which there is no failure, σ_c is the characteristic stress, and m is the Weibull modulus. The probability of failure for a specimen at each stress level was computed by using the estimator in Equation (4) where P_n is the probability of failure of n^{th} specimen and N is the total number of specimens tested. The cumulative distribution function was rewritten as Equation (5) to obtain m, σ_c and σ_u from the Weibull probability plot shown in Figure 5. The m, σ_c and σ_u were calculated for both the two and three parameter Weibull distribution and are provided in Table 2. The characteristic strengths for each type of specimen calculated from the Weibull analysis using the two and the three parameter analysis were identical. The Weibull modulus of columnar polysilicon was 50% larger than that of laminated polysilicon indicating that the defects causing failure of columnar polysilicon are of very consistent size and location. This consistency in the value of Weibull modulus of columnar polysilicon implies that the relevant catastrophic flaws were potentially introduced during post-processing such as RIE

rather than being random flaws owed to the material grain structure developed during deposition. The latter are commonly surface roughness related flaws and result in Weibull moduli of the order of 10 or lower.

$$P = 1 - \exp\left(-\left(\frac{\sigma - \sigma_u}{\sigma_c} \right)^m \right) \tag{3}$$

$$P_n = \frac{n - 0.5}{N} \tag{4}$$

$$\ln\left(-\left(1 - P\right)\right) = m \ln\left(\frac{\sigma - \sigma_u}{\sigma_c} \right) \tag{5}$$

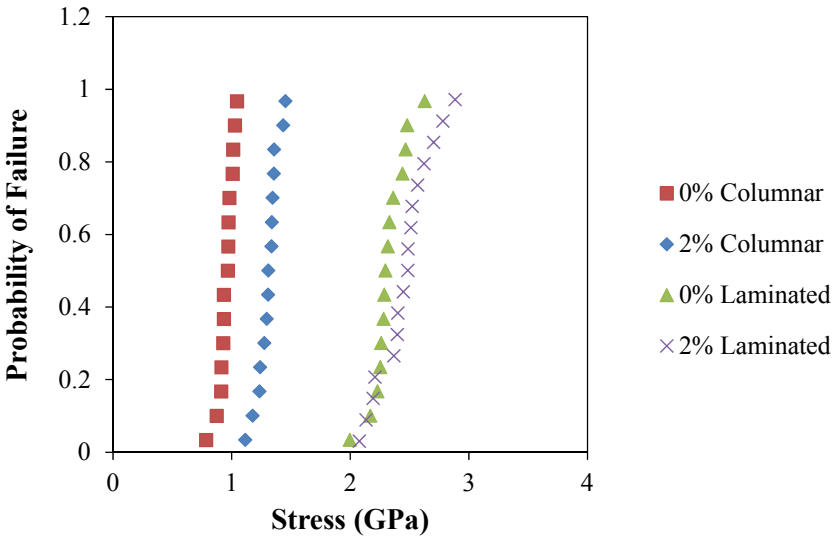

Figure 5. Probability of failure vs. tensile strength for different polysilicon films.

Table 2. Weibull strength and modulus of polysilicon calculated using two and three parameters.

Specimen	2 parameter Weibull		3 parameter Weibull		
	σ_c (GPa)	m	σ_c (GPa)	m	σ_u (GPa)
Undoped, Laminated	2.32	10.31	2.38	6.76	1.45
2% PSG, Laminated	2.51	9.09	2.55	8.36	0.9
Undoped, Columnar	1.34	17.63	1.34	9.31	0.6
2% PSG, Columnar	1.01	16.89	0.98	13.15	0.2

IV. DISCUSSION

IV.a Effect of Grain Structure Fracture and Strength

The effective mode I critical stress intensity factor of undoped polysilicon films was in agreement with the values reported by this group before for MUMPs polycrystalline silicon in the range of 0.8-1.2 MPa√m [24,25]. Due to its polycrystalline nature, the location of the initial crack tip generated in the specimens is expected to reside either inside a grain or at a grain boundary. In [24,25] it was reported that grain boundaries can result in increased apparent mode I critical stress intensity factor. However, three dimensional effects can overshadow such conclusions stemming from 2D material considerations. For instance, Figures 6(a) and 6(b) show AFM images of two different specimens belonging to the same die but exhibiting $K_{IC,eff}$ values of 0.88 MPa√m and 1.03 MPa√m, with the crack tip residing at a grain boundary and inside a grain, respectively.

The scatter in $K_{IC,eff}$ values for undoped columnar polysilicon was higher than that of laminated polysilicon, as shown in Figure 3. This was due to the random distribution of columnar grains with different texture where K_{IC} was dependent on one particular grain lying ahead of the crack tip. On the contrary, the crack tip resided in many grains along the thickness of laminated polysilicon, which resulted in effective K_{IC} that averaged the local K_{IC} of several grains through the specimen thickness. Due to sampling of multiple grains along the crack front, the $K_{IC,eff}$ of laminated polysilicon was close to the average critical stress intensity factor for silicon (~0.9 MPa√m) and resulted in a smaller variation in the measured $K_{IC,eff}$ values.

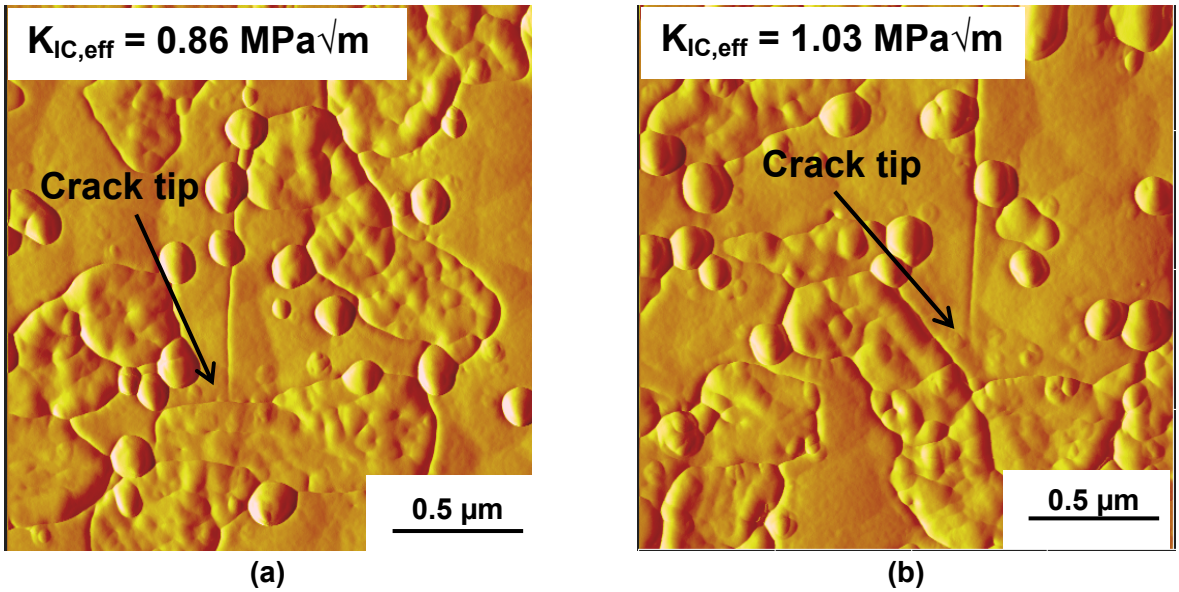

Figure 6. AFM images of columnar polysilicon with crack tip located **(a)** at a grain boundary, and **(b)** within a grain.

Similarly to a previous report on MUMPs polysilicon [24], one of the columnar polysilicon fracture specimens which was doped with 2% PSG, showed subcritical crack growth: after an initial advancement, the crack arrested at a grain boundary and reinitiated at higher load. Figure 7(a) shows a pre-crack extending to the right hand side, and the fracture cross-section in Figure 7(b). The AFM image in Figure 7(d) shows the initial location of the crack tip. Upon an applied load of 5.15 mN, the pre-crack advanced through a grain at an angle with respect to the far field load and arrested at the next grain. A drop in the load is noticed in the force vs. time plot in Figure 7(c). The initial advance critical stress intensity factor was 0.82 MPa$\sqrt{m}$, which lies at the low bound of measured $K_{IC,eff}$ values. The crack resisted further loading up to 6.8 mN when the crack propagated catastrophically for $K_{IC,eff}$ = 1.1 MPa$\sqrt{m}$ which is 25% higher than that for the first crack advance. This R-curve behavior is generated by local variations in strength and toughness due to the inhomogeneous polycrystalline microstructure, as illustrated by the cohesive zone microstructural model [26,27]. In addition to local variations in toughness, it should be noted that the arrested kinked crack in Figure 7(b) required larger far field force to reinitiate catastrophically due to local mode mixity which resulted in higher apparent K_{IC} value.

The Weibull strengths of columnar and laminated polysilicon specimens were 1-1.3 GPa and 2.3-2.5 GPa, respectively. For the same custom polysilicon films, Boyce *et al* [30] reported that characteristic strengths of columnar and laminated polysilicon of 1.76 GPa and 2.80 GPa, respectively, showing the same trend that the laminated polysilicon is substantially stronger than the columnar counterpart. The strength values reported in that previous work are 15-35% higher than that reported here due to Weibull sampling size effects: those previous samples were 180 times smaller (~150×3.74×1 μm^3) leading to higher strengths. The consistency between the two data sets from large and small specimens is examined quantitatively in a later Section of this Final Progress Report.

The large (80%) difference in tensile strength between laminated and columnar microstructures was not due to substantial differences in fracture toughness for the two microstructures, since their toughness values were nearly identical. Instead, the cause of the large strength differences was attributed to process related flaws such as sidewall roughness, grain boundary grooves and holes present on the surface of columnar polysilicon as shown in Figures 8(a,b). The sidewall surface and the top surface of laminated polysilicon was smooth as shown in Figures 8(c) without evident grain boundary grooves and holes. Boyce *et al* reported that the top surface roughness of laminated polysilicon was 20% lower than columnar polysilicon [30], which increased the resistance to fracture of former by 60%. Such variation in average roughness does not entirely explain the large difference in tensile strength; instead one must look for individual defects in the entire specimen surface such as those shown in Figures 8(a,b). Such flaws are possible during post processing, while defects formed during deposition process are expected to be smaller in size.

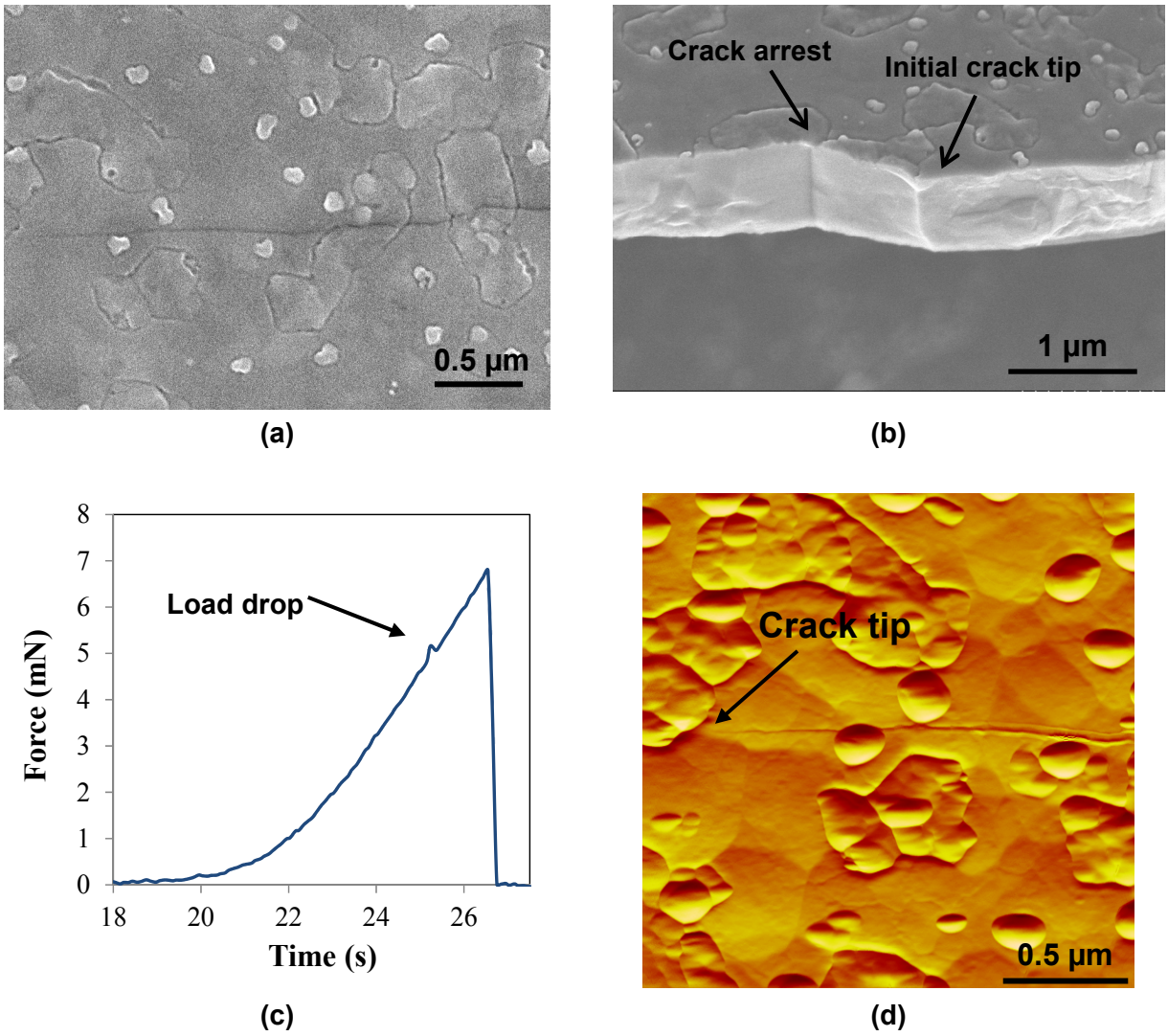

Figure 7. **(a,b)** SEM image of fracture cross sections and top view of the crack in heavily doped columnar polysilicon, **(c)** far-field force vs. time during loading, and **(d)** pre-crack tip.

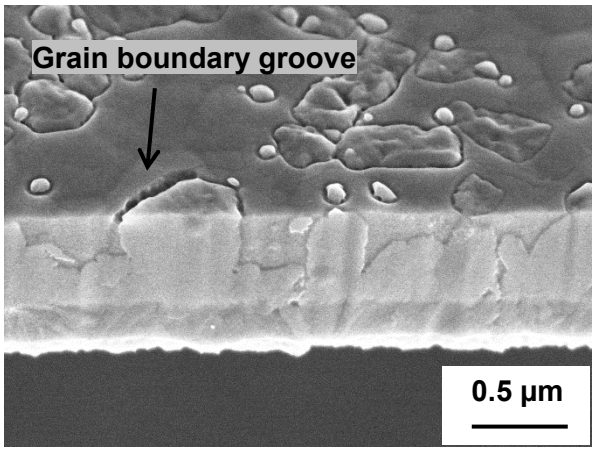

(a)

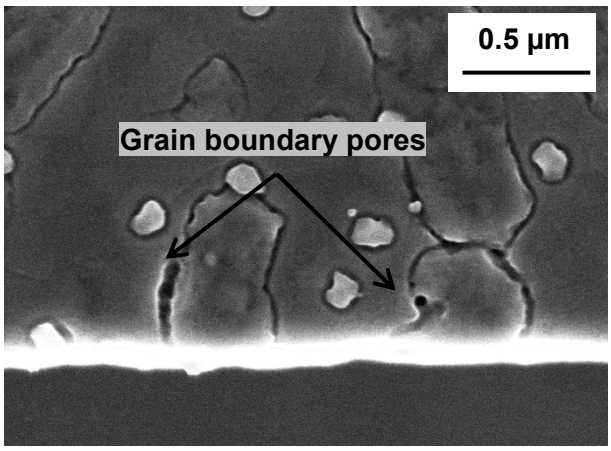

(b)

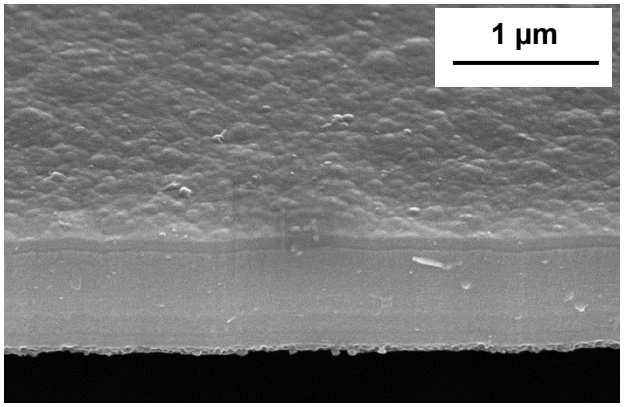

(c)

Figure 8. SEM images showing the side wall and the top surface of **(a,b)** undoped columnar, and **(c)** undoped laminated polysilicon.

IV.b Effect of Doping on Strength and Fracture

The $K_{IC,eff}$ of columnar polysilicon doped with 0.5% and 2% PSG content was 1.02±0.13 MPa√m and 1.05±0.14 MPa√m, respectively. The $K_{IC,eff}$ values of these doped columnar polysilicon films were 10% higher than that of undoped polysilicon of 0.95±0.08 MPa√m. The standard deviation of measured values was also higher for doped polysilicon. During diffusion doping at high temperature (at 1050 °C), P atoms diffuse into the substitutional sites of a Si crystal [28], which can alter the cohesive law of Si thereby affecting the intrinsic critical stress intensity factor. The bond strength of P-Si (363.6 $KJmol^{-1}$) is 11% higher than that of Si-Si (326.86 $KJmol^{-1}$) and hence the energy release rate for polysilicon doped with P is higher than undoped Si [35]. The $K_{IC,eff}$ of doped columnar polysilicon was most frequently in the range of 1.1-1.2 MPa√m. These relatively high $K_{IC,eff}$ values compared to the undoped material were due to the combined effect of crack tip material anisotropy and doping. During doping the P atoms segregate mainly at grain boundaries as the diffusion is higher through them compared to Si grains and hence the intrinsic toughness of Si grain boundaries increases. The presence of tougher grain boundaries in front of crack tip can cause crack arrest or local crack tip deflection that will increase the $K_{IC,eff}$ of the material. It is possible that the true effect of doping on $K_{IC,eff}$ is overshadowed by the critical stress intensity factor dependence on the location of crack tip which already varies in the broad range of 0.8-1.2 MPa√m. On the other hand, the average $K_{IC,eff}$ for laminated doped polysilicon was close to that of undoped polysilicon. In case of laminate polysilicon, the silicon grains present in the outer laminate layers may shadow the grain boundaries of inner laminate layer from diffusion doping. Moreover, due to laminate nature of this material, the crack tip resides at both grains and grain boundaries along film thickness. As a result, the $K_{IC,eff}$ of laminated doped polysilicon did not affect due to doping. As mentioned before, due to differences in grain size, the $K_{IC,eff}$ of laminated polysilicon sampled several grains across the crack plane and hence was lower compared to columnar polysilicon.

Contrary to the small effect on $K_{IC,eff}$, doping had significant impact on the tensile strength of columnar polysilicon, which was 30% lower than that of the undoped material. Large defects, such as crevices and deep grain boundary grooves were evident on the sidewalls and the top specimen surface of doped specimens as shown in Figure 9(a); these features were less pronounced on an undoped specimen shown in Figure 9(b). Investigation of the tested specimen surfaces with an SEM revealed the presence of deep crevices at the specimen edges, which were 100-300 nm long. The specimens etched in 49% HF for times sufficient to etch the top 2-μm sacrificial oxide contained the sidewall defects similar to those shown in Figure 9(a), which implies that sacrificial etching was not responsible for those serious crevices. Thus, the defects in Figure 9(a) could have originated in P diffusion and subsequent annealing processed. On the other hand, no such defects were observed on the surface of doped laminated polysilicon, whose fracture strength was 2.46±0.22 GPa and was not influenced by doping. The Weibull analysis results in Table 2 indicates that the characteristic strength of laminated polysilicon was higher than that of columnar material due to smaller critical defects. However, the Weibull modulus of the former was lower compared to that of the latter revealing that critical flaw sizes were more random in laminated polysilicon. The characteristic strength determined using the three parameter Weibull analysis was very close to that using a two parameter analysis.

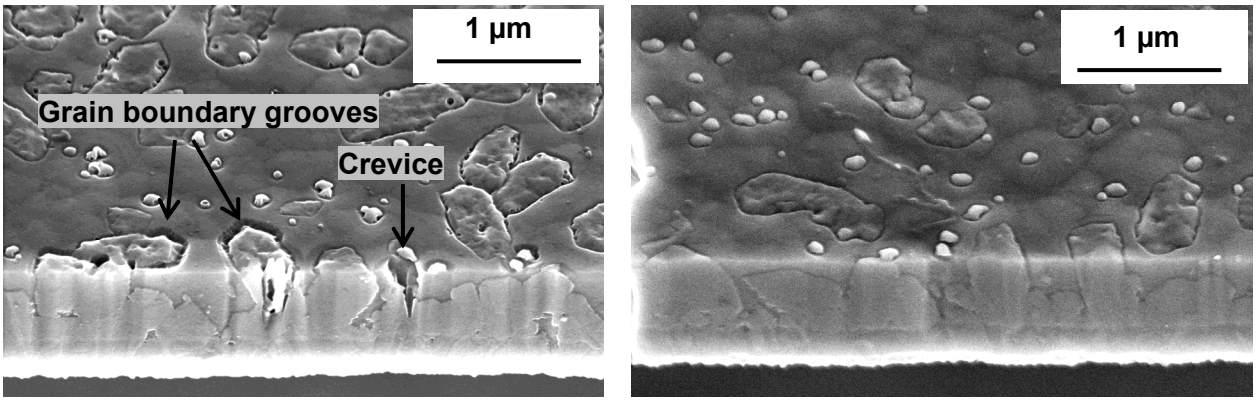

Figure 9. Top surface and side wall of **(a)** doped, and **(b)** undoped columnar polysilicon after etching by 49% HF.

IV.c Scaling of Specimen Size Effect on Tensile Strength

The measured strength of brittle materials depends on the size of the specimens tested. Increasing the specimen size enhances the probability of larger critical flaws present in a specimen and reduces the measured strength. Table 3 compares the characteristic strength and the Weibull modulus of polysilicon measured in this research program with those reported in [30] from specimens that were 180 times smaller in volume. The characteristic strength of both columnar and laminated polysilicon decreased with increased specimen size, as expected. Even though the Weibull modulus of columnar polysilicon increased by 40-90% indicating that the critical flaws were more evenly distributed in bigger specimens, it did not show a particular trend for laminated polysilicon. The consistency of the Weibull parameters extracted from the two specimen sizes in this work and in [30] was evaluated with:

$$\sigma_{c,1} = \sigma_{c,2}\left(\frac{V_2}{V_1}\right)^{\frac{1}{m_2}} \tag{6}$$

$$\sigma_{c,1} = \sigma_{c,2}\left(\frac{A_2}{A_1}\right)^{\frac{1}{m_2}} \tag{7}$$

The characteristic strength of large specimens was estimated using the Weibull parameters measured from small specimens and *vice versa*, assuming that the critical flaws are

distributed in the (a) entire volume, (b) the top specimen surface, and (c) the sidewall surface area. The results are presented in Figure 10. Unfortunately, this analysis cannot distinguish between volumetric critical flaws and top surface area critical flaws because the thickness of specimens was constant for both studies at 1 μm.

Table 3. Weibull parameters of polysilicon measured in this project and by Boyce et al. [30].

Specimen	This work Dimensions – 1000×100×1 μm^3		Boyce *et al* [30] Dimensions ~ 150×3.75×1 μm^3	
	σ_c (GPa)	m	σ_c (GPa)	m
Undoped, Laminated	2.32	10.31	2.80	8.6
2% PSG, Laminated	2.51	9.09	2.83	13.5
Undoped, Columnar	1.34	17.63	1.76	12.9
2% PSG, Columnar	1.01	16.89	1.48	8.7

Therefore, an assessment of the severity of volumetric flaws was done by evaluating the Weibull stress and modulus by taking into account the specimen cross-sectional area. This assessment is quite approximate as it does not account for the different in length between the small and the large specimens compared here. The bar charts in Figures 10(a,b) provide support that the Weibull size effect is governed by critical defects residing on or along the specimen sidewall surface, as the σ_c of large specimens can be closely predicted from experimental data from small specimens and *vice versa*. An analysis using the specimen top surface area and the specimen cross-sectional area did not result in as good agreement between the two data sets as shown in Figures 10(c-f). This analysis is further corroborated by our previous discussion and SEM images that fracture initiated by defects on the specimen sidewalls.

Finally, the characteristic strengths of laminated and columnar polysilicon measured in this work and in [30] are compared in Figure 11 with that of the corresponding polysilicon layers fabricated using Sandia's standardized SUMMiT V^{TM} [8] process. As shown, σ_c of the Poly1 layer can be enhanced 40-150% by controlling the microstructure of polysilicon as described in this paper. As a result, if Poly1 were fabricated as a laminated structure, it could have a characteristic strength as high as that of the Poly4 layer which has been reported to be the strongest of all polysilicon layers of the SUMMiT V^{TM} process due to its minimal surface roughness.

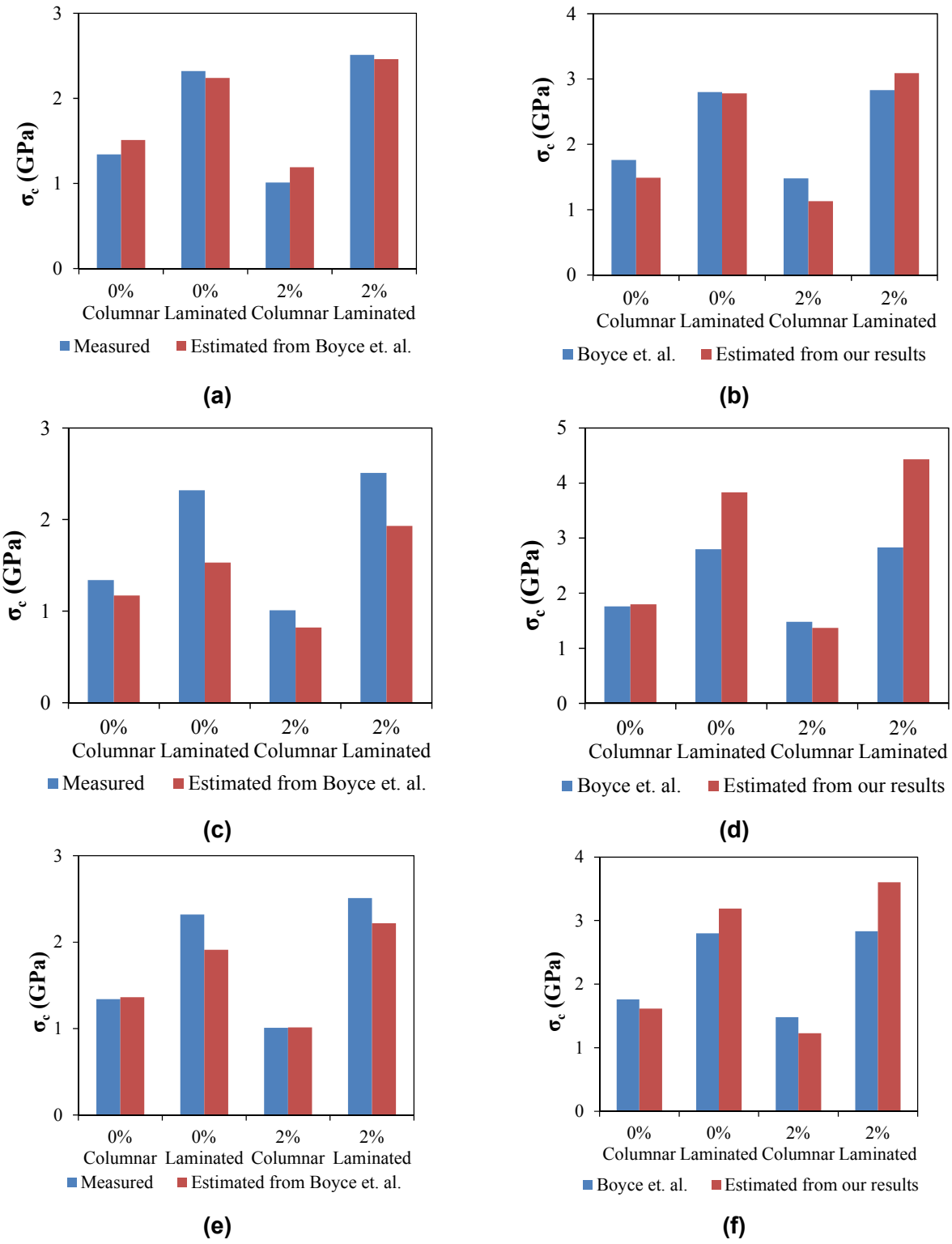

Figure 10. Estimates of characteristic strength of large and small specimens using data from small and large specimens, respectively, assuming that critical flaws lie in the **(a-b)** sidewall area, **(c-d)** top surface area, and **(e-f)** cross-sectional area.

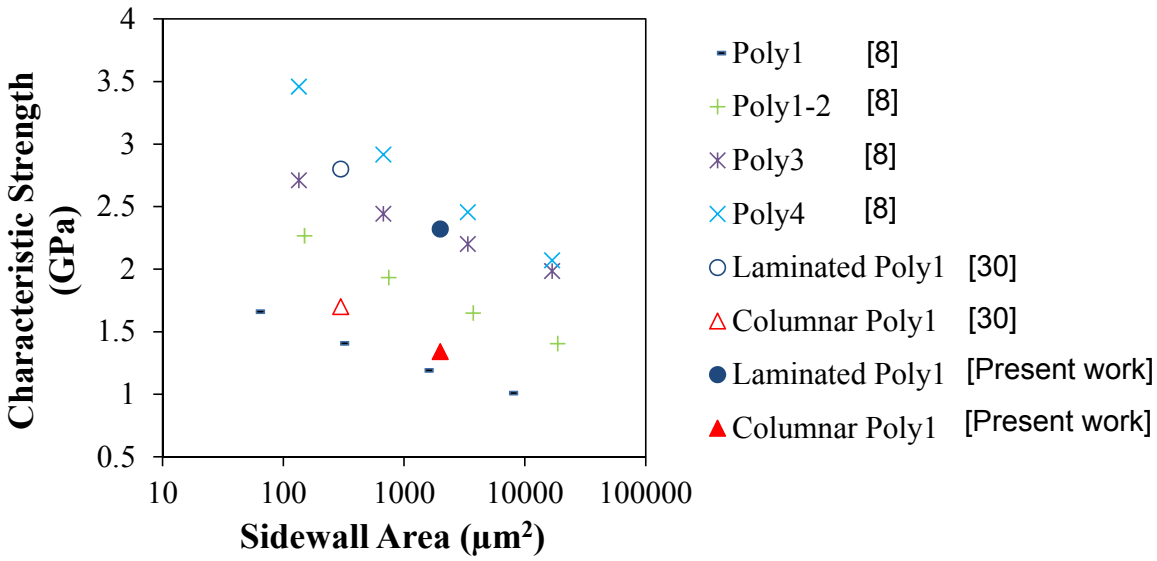

Figure 11. Comparison of characteristic strength of polysilicon measured in this program, with that of the Poly layers fabricated by the standard SUMMiT V™ process. The sidewall area of the specimens tested in this work was 2,000 μm^2. The characteristic strengths of Poly1, Poly1-2, Poly3, Poly4 have been calculated using Equation (7), and Weibull modulus and characteristic strength reported in [8] for specimens with gage surface area of 1,000 μm^2.

V. CONCLUSIONS

The effects of microstructure and doping on the mode I critical stress intensity factor and tensile strength of columnar and laminated polysilicon were investigated. The $K_{IC,eff}$ of columnar and laminated polysilicon with different doping conditions was in the range of 0.8-1.2 MPa$\sqrt{m}$. Due to material anisotropy at the crack tip, the $K_{IC,eff}$ varied by as much as 25% from sample to sample for each type of polysilicon. The average $K_{IC,eff}$ of laminated polysilicon was smaller with less scatter than that of columnar polysilicon, which was attributed to differences in the number of grains sampled by the crack tip. Doping caused 10% increase in the average $K_{IC,eff}$ of columnar polysilicon due to the formation of P-Si bonds. However, doping did not have a noticeable effect on laminated polysilicon which had larger boundary area to dilute the dopant content.

While doping lowered the tensile strength of columnar polysilicon by 23%, it had very little effect on the strength of laminated polysilicon. The Weibull modulus of columnar polysilicon was twice as high as that of laminated polysilicon indicating that the defects were more consistent in shape orientation and location. The tested specimens exhibited 15-35% lower strength than specimens with 180 times smaller volume, showing a clear size effect but obeying the same Weibull probability density function: The Weibull parameters calculated from the present experiments could accurately predict the characteristic strength of smaller polysilicon specimens of the same grain size and doping, and *vice versa*. The microstructurally modified columnar and laminated polysilicon resulted in considerably higher strength values compared to the corresponding polysilicon layers fabricated using the standard SUMMiT V^{TM} process by the Sandia National Labs.

VI. REFERENCES

[1] http://mems.sandia.gov/gallery/images.html

[2] A. McCarty, I. Chasiotis, “Description of Brittle Failure of Non-uniform MEMS Geometries”, Thin Solid Films 515, pp. 3267-3276, 2007

[3] F. Ericson, J.A. Schweitz, "Micromechanical fracture strength of silicon", Journal of Applied Physics, 68 (11), pp. 5840-5844, 1990

[4] T. Alan, M.A. Hines, A.T. Zehnder, "Effect of surface morphology on the fracture strength of silicon nanobeams", Applied Physics Letters, 89 (9), Art. no. 091901, 2006

[5] I. Chasiotis, W.G. Knauss, "The mechanical strength of polysilicon films: Part 2. Size effects associated with elliptical and circular perforation", Journal of the Mechanics and Physics of Solids 51 (8), pp. 1551-15, 2003

[6] W. Sharpe Jr., K. Jackson, J. Hemker, Z.Xie, "Effect of specimen size on young's modulus and fracture strength of polysilicon", Journal of Microelectromechanical Systems 10 (3), pp. 317-326, 2001

[7] J. Koskinen, J. Steinwall, R. Soave, H. Johnson, "Microtensile testing of free-standing polysilicon fibers of various grain sizes", Journal of Micromechanics and Microengineering, 3 (1), pp. 13-17, 1993

[8] B.L. Boyce, J.M. Grazier, T.E. Buchheit and M.J. Shaw, "Strength distributions in polycrystalline silicon MEMS", Journal of Microelectromechanical Systems, 16 (2), pp. 179-190, 2007

[9] S.S. Hazra, M.S. Baker, J.L. Beuth, M.P. De Boer, "Demonstration of an in situ on-chip tensile tester", Journal of Micromechanics and Microengineering, 19 (8), art. no. 082001, 2009

[10] E.D. Reedy Jr., B.L. Boyce, J.W. Foulk III, R.V. Field Jr.,M.P. de Boer, and S.S. Hazra, "Predicting fracture in micrometer-scale polycrystalline silicon MEMS structures", Journal of Microelectromechanical Systems, 20 (4), pp.922-932, 2011

[11] W. Sharpe Jr, K. Jackson, K. Hemker, and Z. Xi, " Effect of Specimen Size on Young’s Modulus and Fracture Strength of Polysilicon", Journal of MEMS, 10, pp. 317-326, 2001

[12] I. Chasiotis, “Mechanics of Thin Films and Microdevices”, IEEE Transactions of Devices, Materials, and Reliability 4 (2), pp. 176-188, 2004

[13] I. Chasiotis, W.G. Knauss, “The Mechanical Strength of Polysilicon Films: 1. The Influence of Fabrication Governed Surface Conditions”, Journal of the Mechanics and Physics of Solids 51, pp. 1533-1550, 2003

[14] H. Kahn, C. Deeb, I. Chasiotis, and A.H. Heuer, “Anodic oxidation during MEMS processing of silicon and polysilicon: native oxides can be thicker than you think”, Journal of Microelectromechanical Systems 14 (5), pp. 914-923, 2005

[15] D.C. Miller, B.L. Boyce, P.G. Kotula, and C.R. Stoldt, "Connections between morphological and mechanical evolution during galvanic corrosion of micromachined polycrystalline and monocrystalline silicon", Journal of Applied Physics, 103 (12), 123518, 2008

[16] R. Ballarini, H. Kahn, N. Tayebi, and A.H. Heuer, "Effects of microstructure on the strength and fracture toughness of polysilicon: A wafer level testing approach," ASTM special technical publication, 1413, pp. 37-51, 2001

[17] T. Tsuchiya, J. Sakata and Y. Taga, "Tensile strength and fracture toughness of surface micromachined polycrystalline silicon thin films prepared under various conditions" MRS Symposium Proceedings, 505 , pp. 285-290, 1997

[18] F. Ebrahimi, and L. Kalwani, "Fracture anisotropy in silicon single crystal", Materials Science and Engineering: A, 268 (1-2), pp. 116-126, 1999

[19] C.P. Chen, and M.H. Leipold, "Fracture toughness of silicon", American Ceramics Society Bulletin, 59, pp. 519, 1980

[20] Y. Tsai and J. Mecholsky, "Fractal fracture of single crystal silicon", Journal of Materials Resources 6, pp. 1248–1263, 1991

[21] A.M. Fitzgerald, R.H. Dauskardt and T.W. Kenny, "Fracture toughness and crack growth phenomena of plasma-etched single crystal silicon", Sensors and Actuators A, 83, pp. 194–199, 2000

[22] H. Kahn, N. Tayebi, R. Ballarini, R.L. Mullen, A.H. Heuer, "Fracture toughness of polysilicon MEMS devices", Sensors and Actuators A: Physical, 82 (1-3), pp. 274-280, 2000

[23] J. Bagdahn, J. Schischka, M. Petzold, W.N. Sharpe Jr., "Fracture toughness and fatigue investigations of polycrystalline silicon", Proceedings of SPIE - The International Society for Optical Engineering, 4558, pp. 159-168, 2001

[24] I. Chasiotis, S.W. Cho, K. Jonnalagadda, "Fracture toughness and subcritical crack growth in polycrystalline silicon", Journal of Applied Mechanics 73 (5), pp. 714-722, 2006

[25] S.W. Cho, K. Jonnalagadda, I. Chasiotis, "Mode I and mixed mode fracture of polysilicon for MEMS", Fatigue and Fracture of Engineering Materials and Structures, 30 (1), pp. 21-31, 2007

[26] J.W. Foulk, III, G.C. Johnson, P.A. Klein, and R.O. Ritchie, "A micromechanical basis for partitioning the evolution of grain bridging in brittle materials", Journal of the Mechanics and Physics of Solids, 55 (4), pp. 719-743, 2007

[27] J.W. Foulk, III, G.C. Johnson, P.A. Klein, and R.O. Ritchie, "On the toughening of brittle materials by grain bridging: Promoting intergranular fracture through grain angle, strength, and toughness", Journal of the Mechanics and Physics of Solids, 56 (6), pp. 2381-2400, 2008

[28] Z. Zeng, X. Ma, J. Chen, Y. Zeng, D. Yang, and Y. Liu, "Effects of heavy phosphorus-doping on mechanical properties of Czochralski silicon", Journal of Applied Physics, 107 (12), pp. 123503-1-5, 2010

[29] J. G. Swadener and M. Nastasi, "Effect of dopants on the fracture toughness of silicon", Journal of Materials Science Letters, 21 (17), pp. 1363-1365, 2002

[30] B.L. Boyce, M.J. Shaw, P. Lu, M.T. Dugger, "Stronger silicon for microsystems", Acta Materialia 58, 439–448, 2010

[31] J. J. Sniegowski and M. P. de Boer, "IC-compatible polysilicon surface micromachining", Annual Review of Material Science, 30, pp. 299-333, 2000

[32] K. Jonnalagadda, I. Chasiotis, S. Yagnamurthy, J. Lambros, J. Pulskamp, R. Polcawich, M. Dubey, "Experimental investigation of strain rate dependence of nanocrystalline Pt films", Experimental Mechanics, 50, pp. 25-35, 2010

[33] H. Tada, P. C. Paris, and G. R. Irwin, , The stress analysis of cracks handbook, 3rd ed., ASME Press, New York, pp. 52–53, 2000

[34] A. Hallinan Jr., "A review of the Weibull distribution", Journal of Quality Technology, 25 (2), pp. 85-93, 1993

[35] D.R. Lide, Handbook of chemistry and physics, 85th Ed, CRC Press LLC